Atomic mechanism of zinc-blende to NiAs high-pressure phase transition in BeTe

2008 J. Phys.: Condens. Matter 20 485218

(http://iopscience.iop.org/0953-8984/20/48/485218)

J. Phys.: Condens. Matter **20** (2008) 485218 (6pp) doi:10.1088/0953-8984/20/48/485218

Atomic mechanism of zinc-blende to NiAs high-pressure phase transition in BeTe

Yingxiang Cai[1] **and Rui Xu**[2]

[1] Department of Physics, NanChang University, Jiangxi, Nanchang 330031, People's Republic of China
[2] State Key Laboratory of Metastable Materials Science and Technology, YanShan University, Hebei, Qinhuangdao 066004, People's Republic of China

E-mail: yxcai@yahoo.com

Received 22 July 2008, in final form 7 October 2008
Published 28 October 2008
Online at stacks.iop.org/JPhysCM/20/485218

Abstract

The atomic mechanism of the zinc-blende to NiAs structural transition under high pressure was investigated by crystallographic analysis and first-principles pseudopotential methods within the generalized gradient approximation. The relative sliding of less-close-packed cation layers $\{001\}_C$ along the $\langle 100\rangle$ directions could be identified, accompanied by changes of lattice parameters and the fractional coordinates of anions, briefly referred to as the less-close-packed to most-close-packed cation layer transition mechanism. BeTe was taken as an example to study the changes of lattice parameters, enthalpy difference and the fractional coordinates of anions with the relative sliding of cations at equilibrium transition pressure. Furthermore, the change of the charge density along the transition path was investigated to characterize the formation of two new Be–Te bonds.

(Some figures in this article are in colour only in the electronic version)

1. Introduction

The group IV, III–V and II–VI binary compounds are of both technical and scientific interest due to their numerous structural, electric and optic properties. At ambient temperature and pressure, most of them crystallize into either cubic zinc-blende (ZB) or hexagonal wurtzite (WZ) structure except for some chalcogenides of group IIA, which have the rock-salt (RS) structure. Both theoretical and experimental studies show that these compounds tend to transform to more high-coordinated structures under high pressure, and the four most typical kinds of high-pressure phase transformations from fourfold to sixfold coordinated crystal structures are the ZB to the RS, the WZ to the RS, the ZB to nickel arsenide (NA) and the WZ to the NA. Many experimental studies and theoretical calculations can be found for these kinds of phase transitions [1, 2]. Recently, the research interest has been devoted to elucidating the phase transition mechanism, because by only understanding how one structure transforms into another structure, i.e. the phase transition path or atomic mechanism, we could understand the nature of the high-pressure phase transition. The more profound meaning of the study of the phase transition mechanism is that it may promote the theoretical and experimental study on how to control or manipulate the transition and accordingly synthesize new high-pressure phases. To the best of our knowledge, only the WZ–RS [3–7], the WZ–NA [8] and the ZB–RS [9–13] transition mechanisms have been investigated in detail among the typical phase transitions in $A^{8-N}B^N$ binary compounds up to now. A few mechanisms have been put forward, for instance, the bilayer sliding mechanism for the ZB–RS [9] and homogeneous strain deformation or triaxial strain deformation mechanisms in the WZ–RS [5, 7]. Unfortunately, the problem of the transformation mechanism from the ZB to the NA structure remains unsolved while the ZB–RS, the WZ–RS and the WZ–NA have been well established. Hence, the findings of the WZ–NA mechanism will complete the mechanisms of typical $A^{8-N}B^N$ binary compounds. At present, experimental and theoretical studies have shown that five binary compounds (BeTe [14], BeSe [14], BeS [15], AlAs [16] and AlP [17]) have been found to undergo the ZB–NA structural transition under high pressure. A common feature is that all of them belong to the family of indirect-bandgap semiconductors. Among them, the beryllium chalcogenides (BeS, BeSe and BeTe) have bandgaps (along Γ–X) ranging from 1.80 to 4.17 eV [18–20] and for AlAs and AlP the indirect bandgap is 2.24 eV and

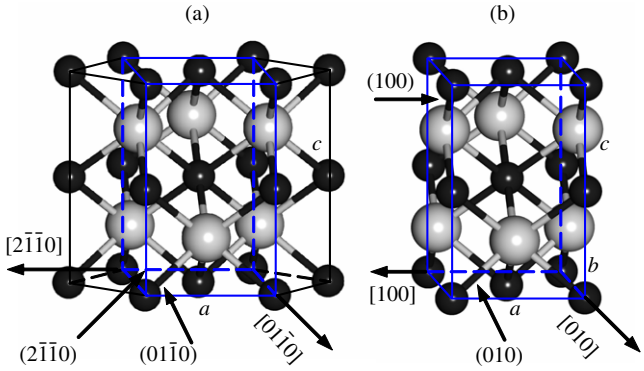

Figure 1. Crystal structure of NA-type BeTe: (a) is a hexagonal cell and (b) is an orthorhombic cell. Light grey spheres denote anions and black spheres are cations.

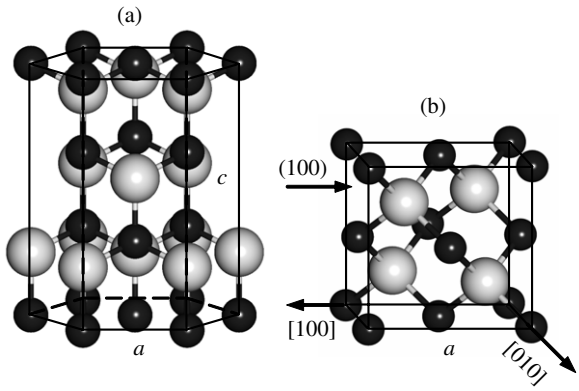

Figure 2. Crystal structure of ZB-type BeTe: (a) is a hexagonal cell and (b) is a cubic cell.

2.52 eV [21], respectively. Furthermore, in terms of chemical bonding, each of these five compounds has a small Phillips ionicity value $f_i \leqslant 0.312$ [22].

In this paper, we took BeTe ($f_i = 0.169$) as an example to investigate the ZB–NA transition mechanism. By means of crystallographic analysis, a possible transition path from the ZB to the NA structure was proposed firstly. Then, a first principle pseudopotential method was used to confirm the validity of the transform mechanism. The lattice parameters and the phase transition barrier were determined as well. In addition, the change of the charge density in the sliding plane along the transition path was monitored and thereby the forming of two new chemical bonds was characterized.

2. Crystallographic analysis and computational method

Firstly, the crystal structures of the ZB and the NA should be analysed in detail. The NA structure belongs to the space group P63/mmc with two formula units per primitive cell. The stacking sequence of atoms is ABAC$\cdots$ in the $[0001]_{\mathrm{H}}$ direction of the hexagonal cell as shown in figure 1(a). The A denotes Be atoms and the B and C are Te atoms. In general, a hexagonal cell is used to characterize the NA structure. However, an orthorhombic cell, as shown in figure 1(b), will be adopted in the following study of the phase transition mechanism and theoretical calculations. Its underlying advantage is that it is easy to discover the inherent correlation between the ZB and the NA structures. The orthorhombic cell of the NA-type BeTe can be obtained by cutting the hexagonal cell using $(2\bar{1}\bar{1}0)_{\mathrm{H}}$ and $(01\bar{1}0)_{\mathrm{H}}$ planes. The corresponding crystallographic relations between the hexagonal and the orthorhombic cells are $[2\bar{1}\bar{1}0]_{\mathrm{H}} \parallel [100]_{\mathrm{O}}$, $[01\bar{1}0]_{\mathrm{H}} \parallel [010]_{\mathrm{O}}$, $(2\bar{1}\bar{1}0)_{\mathrm{H}} \parallel (100)_{\mathrm{O}}$ and $(01\bar{1}0)_{\mathrm{H}} \parallel (010)_{\mathrm{O}}$. As for the ZB structure, it belongs to space group $F\bar{4}3m$. The stacking sequence of cation–anion dimers is ABCABC$\cdots$ in the $[0001]_{\mathrm{H}}$ direction of the hexagonal cell, as shown in figure 2(a). Usually, the ZB structure is characterized by using a cubic cell as shown in figure 2(b). The most-close-packed planes of cations in the cubic ZB cell are $\{111\}_{\mathrm{C}}$. We define a parameter η, which is used to characterize the degree of tightness of cation stacking in a plane.

$$\eta = \frac{\text{total projected area of cations in two dimensional cell}}{\text{area of two dimensional cell}}.$$

If the rigid sphere model is applied, η in the cubic ZB cell is $\frac{\pi}{2\sqrt{3}}$, $\frac{\pi}{4\sqrt{2}}$ and $\frac{\pi}{8}$ for $\{111\}_{\mathrm{C}}$, $\{011\}_{\mathrm{C}}\{001\}_{\mathrm{C}}$, respectively. Therefore, the $\{001\}_{\mathrm{C}}$ and $\{002\}_{\mathrm{C}}$ represent less-close-packed cation layers. Comparing the orthorhombic NA cell with the cubic ZB cell, we easily find a path along which the ZB structure can continuously transform into the NA structure without any chemical bond breaking.

Table 1. Fractional coordinates (x, y, z) of Te atoms in cubic zinc-blende and orthorhombic NiAs cell.

	Fractional coordinates	
	Cubic ZB cell	Orthorhombic NA cell
Te_1	$(\frac{1}{4}, \frac{1}{4}, \frac{3}{4})$	$(\frac{1}{2}, \frac{1}{6}, \frac{3}{4})$
Te_2	$(\frac{1}{4}, \frac{3}{4}, \frac{1}{4})$	$(\frac{1}{2}, \frac{5}{6}, \frac{1}{4})$
Te_3	$(\frac{3}{4}, \frac{1}{4}, \frac{1}{4})$	$(1, \frac{1}{3}, \frac{1}{4})$
Te_4	$(\frac{3}{4}, \frac{3}{4}, \frac{3}{4})$	$(1, \frac{2}{3}, \frac{3}{4})$

Figure 3 demonstrates the transition path at the atomic scale. We first compare the fractional coordinates of the cations in the cubic ZB (figure 3(a)) with those of the orthorhombic NA cells (figure 3(e)). It can be found that, for all cations in both structures except for those in the (002) plane, their fractional coordinates are correspondingly equal. If the cations in the $(002)_{\mathrm{C}}$ plane of the ZB structure slide along the $[100]_{\mathrm{C}}$ direction and the increment of their fractional coordinates is equal to 0.5, the fractional coordinates of all cations are identical with those of the orthorhombic NA structure. Next, we consider the anions, which are numbered as Te_1, Te_2, Te_3 and Te_4, respectively, as shown in figure 3(a), and their fractional coordinates are listed in table 1. It can be deduced that the anions will move along the same sliding direction as the cations due to the Be–Te interaction. When the four anions adjust their position and their fractional coordinates are correspondingly equal to those of the orthorhombic NA cell as listed in table 1, the phase transition has finished. In

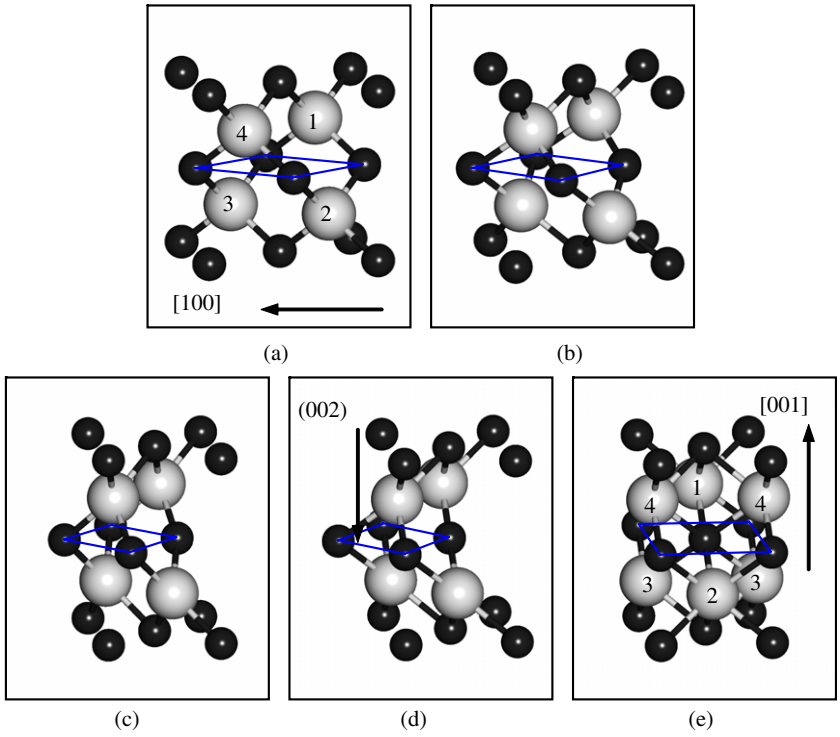

Figure 3. Transitional path from ZB-type to NA-type BeTe. The sliding plane and direction are (002) and [100], respectively. (a) is the ZB structure; (e) is the NA structure; (b), (c) and (d) are intermediate states.

addition, in the course of cation and anion sliding, it can be expected that the lattice parameters will also change in order to maintain enthalpy minimization from the point of view of thermodynamics. Figures 3(b)–(d) represent three intermediate states which are obtained by means of structural optimizations. All of them belong to orthorhombic space group $C222_1$, which stems from a slight distortion of the ZB structure. Hence, the ZB $\rightleftharpoons$ NA transition associates with the space group change of $F\bar{4}3m \rightleftharpoons C222_1 \rightleftharpoons P63/mmc$. Obviously, this transition path is not accompanied by any Be–Te bond breaking. Although there are some other possible transition paths, we find that all of them will suffer from a higher transitional barrier because of the breaking of some Be–Te bonds. Thus such transitions rarely occur in reality.

Secondly, we examined whether the ZB structure can transform into the NA structure or not in accordance with the above transition path. Therefore, we should perform total energy calculations to determine the equilibrium transition pressure (p_e) at which the enthalpies of the ZB-type and the NA-type BeTe are the same, i.e. $H_{ZB} = H_{NA}$, and then carry out structural optimizations at p_e to ascertain the changing history of all structural parameters. All theoretical calculations were performed within the framework of density of functional theory (DFT) with the CASTEP code [23]. Ultrasoft pseudopotentials were expanded within a plane wave basis set with a cut-off energy of 380 eV. We used the generalized gradient approximation (GGA) in the scheme of Perdew–Burke–Ernzerhof (PBE) [24] to describe the exchange and correlation potential because it is more robust than the local density approximation (LDA) in the study of high-pressure phase transition [25–27]. The **k**-point separations in each of the three reciprocal lattice directions were around 0.04(1/Å). The calculations were considered to be converged when the energy difference was below 10^{-7} eV/atom and stress was less than 10^{-4} GPa. During the structural optimizations, only the cation with fractional coordinates (0, 0, 0) was fixed and other cations and anions allowed to relax their atomic positions. Tentative calculations showed that the structure remained orthorhombic. Hence, we constrained the cell angles $\alpha = 90°$, $\beta = 90°$ and $\gamma = 90°$ prior to structural optimizations with the aim of reducing the calculating time. Furthermore, in order to facilitate the description of the transitional path and perform structural optimizations, we defined a sliding parameter ξ, which was the increment of the fractional coordinates of the cations in the (002) plane.

3. Results and discussion

The calculated results show that, at zero pressure, the lattice parameter of the ZB-type BeTe is $a = 5.616$ Å, which is in good agreement with the experimental value (5.617 Å) [14]. Two different strategies are commonly used for determining the transition pressure p_e. One is minimizing the total energy with respect to the structural parameters at constant volume. The common tangent of two total energy–volume curves will give p_e. The other is directly minimizing the enthalpy at constant pressure. The two enthalpy–pressure curves cross at p_e [2]. The latter is adopted in this paper. Figure 4 shows the enthalpies of the ZB- and the NA-type BeTe as a function of pressure. p_e can be obtained from the crossing of two enthalpy

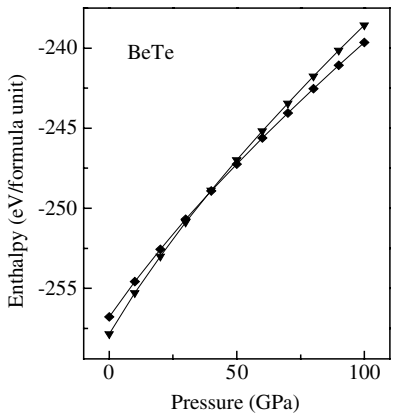

Figure 4. Enthalpy per formula unit as a function of pressure: the solid diamond denotes the enthalpy of NA-type BeTe and the solid down triangle is the enthalpy of ZB-type BeTe.

curves and it is about 36.5 GPa, which agrees very well with the experimental value of 35 GPa [14]. In contrast with the previous study by Muñoz *et al*, which predicted that p_e was ∼32 GPa, our study confirms again that the GGA is more robust than the LDA in the determination of the transitional pressure. At p_e, the lattice parameters are $a = 5.033$ Å for the ZB-type cell, and $a = 3.407$ Å, $b = 5.944$ Å, $c = 5.582$ Å for the orthorhombic NA-type cell. The c/a ratio of the NA-type BeTe is 1.638 and somewhat larger than the ideal value 1.633 or $\sqrt{8/3}$ [2]. Next we optimize the crystal structure for different ξ with an interval of 0.05 at p_e. Figure 5(a) shows the change of the lattice parameters a, b and c as a function of the increment of ξ. It is obvious that a decreases and b and the c increase slowly when ξ increases from 0 to 0.2. Then, in the range of 0.2 to 0.3 for ξ, three lattice parameters abruptly change. While ξ is more than 0.3, a, b and c smoothly approach 3.407 Å, 5.944 Å and 5.582 Å, respectively. They are the lattice constants of the orthorhombic NA cell at p_e. Hence, the results from structural optimizations confirm that the ZB-type BeTe can continuously transform into the NA structure with ξ changing from 0 to 0.5. In view of the special lattice parameter changing (a ↓, b and c ↑), uniaxial compression, i.e. loading pressure on the a axis of a single crystal, might be a more effective type of applied stress to achieve this kind of phase transition. The volume change with ξ is shown in figure 5(b) resulting from the change in lattice parameters with the structure remaining orthorhombic throughout. The relative volume decrease, $(V_{ZB} - V_{NA})/V_{ZB}$, is about 11.35% at p_e. From the abrupt changes of the lattice parameters and the volume at $\xi = 0.2$–0.3, it can be deduced that the phase transition barrier is located in this range. Figure 5(c) shows the transitional barrier ($\triangle H = H - H_{ZB} = H - H_{NA}$) as a function of ξ, where H is the enthalpy per formula unit along the transition path. Its height is estimated to be about 0.23 eV/BeTe while ξ is equal to 0.225. The increasing of ξ or the sliding of the cations in (002) definitely impels the anions to adjust their position in the cell to retain enthalpy minimization. For example, the fractional coordinates x, y and z of Te_4 are $\frac{3}{4}$, $\frac{3}{4}$ and $\frac{3}{4}$ at $\xi = 0$. When ξ is equal to 0.5, the corresponding coordinates change to 1, $\frac{2}{3}$ and $\frac{3}{4}$, as shown in figure 5(d). The above mentioned numerical results show that the relative sliding between (002) and (001) cation layers in the ZB cell finally result in the ZB–NA phase transition. Actually, the ZB–NA transitional mechanism is the transitional course of the less-close-packed planes of the ZB structure to the most-close-packed planes of the hexagonal cell of the NA structure. Based on our recent study [8], it can be found that the transitional mechanism of ZB–NA obviously differs from that of WZ–NA. As for the WZ–NA, the sliding planes of cations stay the most close packed before and after phase transition.

Finally, we monitor the change of the charge density along the aforementioned phase transition path. Figure 6 shows the charge density contours in the (002) plane for five different ξ at p_e. The ZB-type BeTe ($\xi = 0.0$) is more covalent because

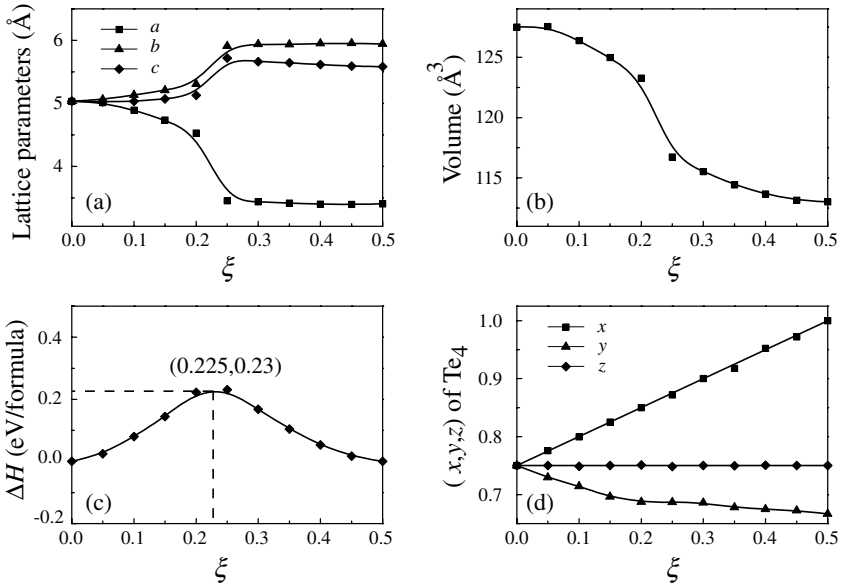

Figure 5. Lattice parameters (a), volume (b), enthalpy difference (c) and fractional coordinates of Te_4 (d) as a function of ξ, respectively.

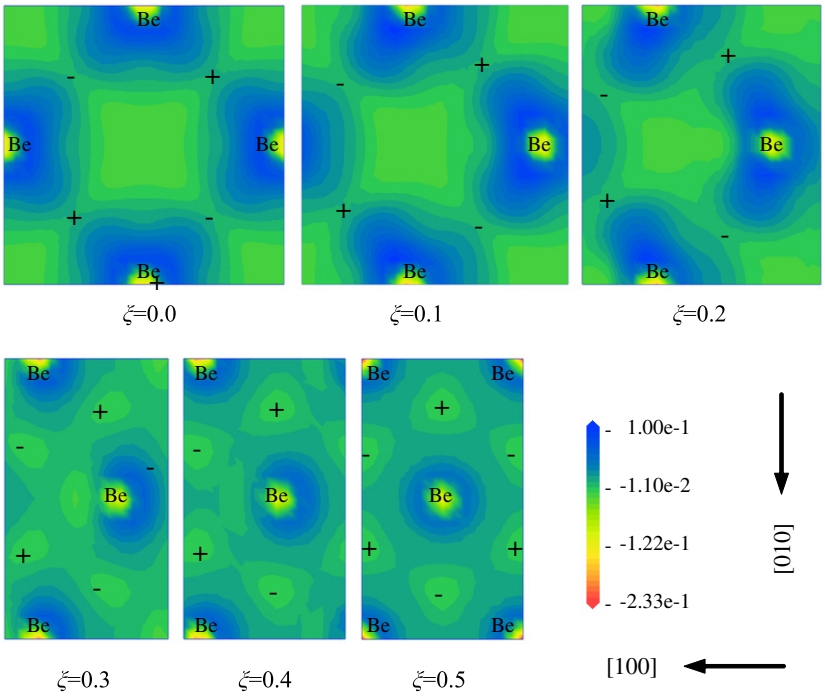

Figure 6. Change of charge density contour with ξ in the sliding plane. The + and − signs denote the Te atoms lying above and below the sliding plane, respectively.

its charge density contour tends to be a square shape. The charge density distribution reflects that each cation combines with four anions. In contrast, the NA-type BeTe ($\xi = 0.5$) is more ionic because the charge density contour is inclined to be a spherical shape, and the charge density distribution shows that each cation combines with six anions. However, more attention should be given to the charge density contours at $\xi = 0.2$ and $\xi = 0.3$. It is clear that an abrupt change of the charge density occurs in this region. This is just the result of the formation of two new Be–Te bonds without breaking any old ones in order to decrease the total energy. In another words, a more covalent compound transforms into a more ionic compound while ξ increases from 0.2 to 0.3.

4. Conclusions

In conclusion, the mechanism of high-pressure phase transformation from zinc-blende to NiAs structure has been investigated at the atomic scale by means of crystallographic analysis and DFT calculations. It is the relative sliding of $\{001\}_C$ less-close-packed cation layers along the $\langle 100 \rangle$ directions accompanied by the changes of the lattice parameters and the fractional coordinates of anions. Meanwhile, the space group degrades to $C222_1$ during the phase transition. This mechanism has been applied to the phase transformation in BeTe and the enthalpy barrier (0.23 eV/BeTe) has been determined by the first-principles density functional theory calculations. In addition, the analysis of charge density changing reflects the course of formation of two new chemical bonds. We expect that this mechanism can be applied to other binary compounds (such as BeS, BeSe, AlP, AlAs) which undergo similar high-pressure phase transition.

Acknowledgment

This project was supported by the Research Foundation of JiangXi Provincial Department of Education (grant No GJJ08063).

References

[1] Ackland G J 2001 *Rep. Prog. Phys.* **64** 483
[2] Mujica A, Rubio A, Muñoz A and Needs R J 2003 *Rev. Mod. Phys.* **75** 863
[3] Limpijumnong S and Lambrecht W R L 2001 *Phys. Rev.* B **63** 104103
[4] Limpijumnong S and Jungthawan S 2004 *Phys. Rev.* B **70** 054104
[5] Cai Y, Wu S, Xu R and Yu J 2006 *Phys. Rev.* B **73** 184104
[6] Shimojo F, Kodiyalam S, Ebbsjö I, Kalia R K, Nakano A and Vashishta P 2004 *Phys. Rev.* B **70** 184111
[7] Limpijumnong S and Lambrecht W R L 2001 *Phys. Rev. Lett.* **86** 91
[8] Cai Y, Wu S, Yu J and Xu R 2006 *Phys. Rev.* B **74** 214112
[9] Hatch D M, Stokes H T, Dong J, Gunter J, Wang H and Lewis J P 2005 *Phys. Rev.* B **71** 184109
[10] Shimojo F, Ebbsjö I, Kalia R K, Rino J P and Vashishta P 2000 *Phys. Rev. Lett.* **84** 3338
[11] Catti M 2001 *Phys. Rev. Lett.* **87** 035504
[12] Miao M S and Lambrecht W R L 2005 *Phys. Rev. Lett.* **94** 225501
[13] Miao M S and Lambrecht W R L 2003 *Phys. Rev.* B **68** 092103
[14] Luo H, Ghandehari K, Greene R G and Ruoff A L 1995 *Phys. Rev.* B **52** 7058
[15] Narayana C, Nesamony V J and Ruoff A L 1997 *Phys. Rev.* B **56** 14338
[16] Greene R G, Luo H, Li T and Ruoff A L 1994 *Phys. Rev. Lett.* **92** 2045

[17] Greene R G, Luo H and Ruoff A L 1994 *J. Appl. Phys.* **76** 7296
[18] Yim W M, Dismukes J P, Stofko E J and Paff R J 1972 *J. Phys. Chem. Solids* **33** 501
[19] González-Díaz M, Rodríguez-Hernández P and Muñoz A 1997 *Phys. Rev.* B **55** 14043
[20] Stukel D J 1970 *Phys. Rev.* B **2** 1852
[21] Vurgaftman I, Meyer J R and Ram-Mohan L R 2001 *J. Appl. Phys.* **89** 5815
[22] Phillips J C 1970 *Rev. Mod. Phys.* **42** 317
[23] Segall M D, Lindan P J D, Probert M J, Pickard C J, Hasnip P J, Clark S J and Payne M C 2002 *J. Phys.: Condens. Matter* **14** 2717
[24] Perdew J P, Burke K and Ernzerhof M 1996 *Phys. Rev. Lett.* **77** 3865
[25] Jaffe J E, Snyder J A, Lin Z and Hess A C 2000 *Phys. Rev.* B **62** 1660
[26] Sun J, Wang H-T, He J and Tian Y 2005 *Phys. Rev.* B **71** 125132
[27] Catti M 2003 *Phys. Rev.* B **68** 100101